Exploring 5-40 AU scales around AB Aurigae with an upgraded Palomar Fiber Nuller

Jonas Kühn*[a], Bertrand Mennesson[a], Kurt Liewer[a], Stefan Martin[a], Frank Loya[a], Rafael Millan-Gabet[b], Eugene Serabyn[a]
[a]Jet Propulsion Laboratory, California Institute of Technology, 4800 Oak Grove Drive, Pasadena, CA 91109-8099, USA; [b]NASA Exoplanet Science Institute, California Institute of Technology, Pasadena, CA 91125, USA

ABSTRACT

With a null precision of a few 10^{-4} at all azimuth angles inside a field-of-view extending from 35 to 275 mas, the Palomar Fiber Nuller (PFN) is able to explore angular scales intermediate between those accessed by coronagraphic imaging and by long baseline interferometry. We first briefly summarize the recent performance improvements of the PFN (sensitivity, azimuthal coverage, duty cycle efficiency on-sky) over the 2011-2014 time period. Then we report on recent K-band observations of the young pre-main sequence star AB Aurigae obtained with the PFN. It is shown that a mean astrophysical null of 1.52% was detected around AB Aur at all probed azimuthal angles, and this inside a field-of-view corresponding to projected separations between 5 and 40 AU. In addition, we also report a slight ±0.2% modulation in addition to this average null level. The isotropic astrophysical null is indicative of circumstellar emission dominated by an azimuthally extended source, possibly a halo or one or more rings of dust. The modest azimuthal variation may be explained by some skewness or anisotropy of the spatially-extended source, e.g. with an elliptical or spiral geometry, or clumping, but it could also be due to the presence of a point-source located at a separation of ~120 mas (17AU) and carrying ~6*10-3 of the stellar flux.

Keywords: Nulling interferometer, Interferometry, AB Aurigae, Herbig star, Planet formation, Protoplanetary disk

1. INTRODUCTION

With current generation instruments, there is still a gap of observational coverage in-between long-baseline interferometry and direct imaging from the ground, i.e. at angular scales between 30 and 100 mas. In the case of nearby stars between 10 to 100 pc this corresponds to projected separations extending from 0.3 – 3 AU to 1 – 10 AU, essentially the highly interesting solar system parameter space. Thanks to an effective search space extending from ~35 mas (inner half transmission point) to ~275 mas (outer half transmission point), the Palomar Fiber Nuller (PFN)[1-4] is ideally suited to provide measurement at these missing scales. Performance-wise, the PFN delivers very deep on-sky nulls (< 0.1%) at K-band, and was already used to derive some of the best constraints on the presence of a companion within 2 AU of Vega.[5] Thanks to recent improvements during the 2011-14 time period presented hereafter, the PFN can now achieve a complete azimuthal coverage at this contrast level for targets brighter than about magnitude 7 at K-band.

Located at 144 pc from us, the young (4 ± 1 Myr) massive ($M \sim 2.4 \pm 0.2 M_{\odot}$[6]) pre-main sequence star AB Aurigae (AB Aur) is considered an ideal prototype for studying planet formation and migration processes. As a member of the Herbig Ae class, AB Aur has been extensively investigated in the near-infrared (NIR), notably by direct and polarimetric imaging,[7-10] as well as long-baseline interferometry (10-350 m baseline lengths).[11-14] The AB Aur system presents a complex picture, probably including unseen ongoing planetary formation processes, at a variety of scales. Here, the current missing gap of observational coverage lies in the solar system scale, ranging from ~5 to 40 AU. This is therefore an ideal target for the PFN, capable of exploring this scale for the first time.

*jonas.g.kuhn@jpl.nasa.gov; phone 1 818 354-0903

Optical and Infrared Interferometry IV, edited by Jayadev K. Rajagopal, Michelle J. Creech-Eakman, Fabien Malbet, Proc. of SPIE Vol. 9146, 914606 • © 2014 SPIE • CCC code: 0277-786X/14/$18
doi: 10.1117/12.2056798 Proc. of SPIE Vol. 9146

2. THE PALOMAR FIBER NULLER (PFN) INSTRUMENT

2.1 Principle

The PFN[1-4] – a rotatable nulling interferometer – is using a single-mode (SM) fiber to combine two destructively-interfered telescope sub-apertures. A schematic of this instrument on the Palomar 200-inch is presented in Figure 1. Essentially, the PFN re-images the Hale Telescope pupil at K-band on a pair of elliptical apertures, while being able to rotate this image by means of an actuated K-mirror. On the sky, this has the effect of rotating an equivalent fixed baseline of b = 3.2 m between a pair of elliptical apertures of 3 x 1.5 m. The J-/H-and visible parts of the spectrum are used for internal alignment purposes, as well as for tracking differential tip/tilt drift between the PALM-3000 (p3k) Adaptive Optics (AO) system and the PFN bench (see §2.3). Downstream of the aperture pair are two piezo-mirrors used for adjusting the Optical Path Difference (OPD) between the beams, as well as for optimizing the injection into the output SM fiber. Then the pair of beams go through a beam-selector chopper wheel (see §2.5) and a chevron-shaped piece of glass on a motorized rotator stage, used for 1) adjusting the differential glass thickness to make the OPD achromatic, 2) bring both beams closer together to optimize the SM fiber injection efficiency. Finally the parallel beams are both coupled into the SM fiber (SM-2000, Thorlabs) by an F/4.5 off-axis parabola, and the fiber output is focused on a single-pixel detector located on the dome floor (infrared detector inherited from the Palomar Testbed Interferometer, see §2.4).

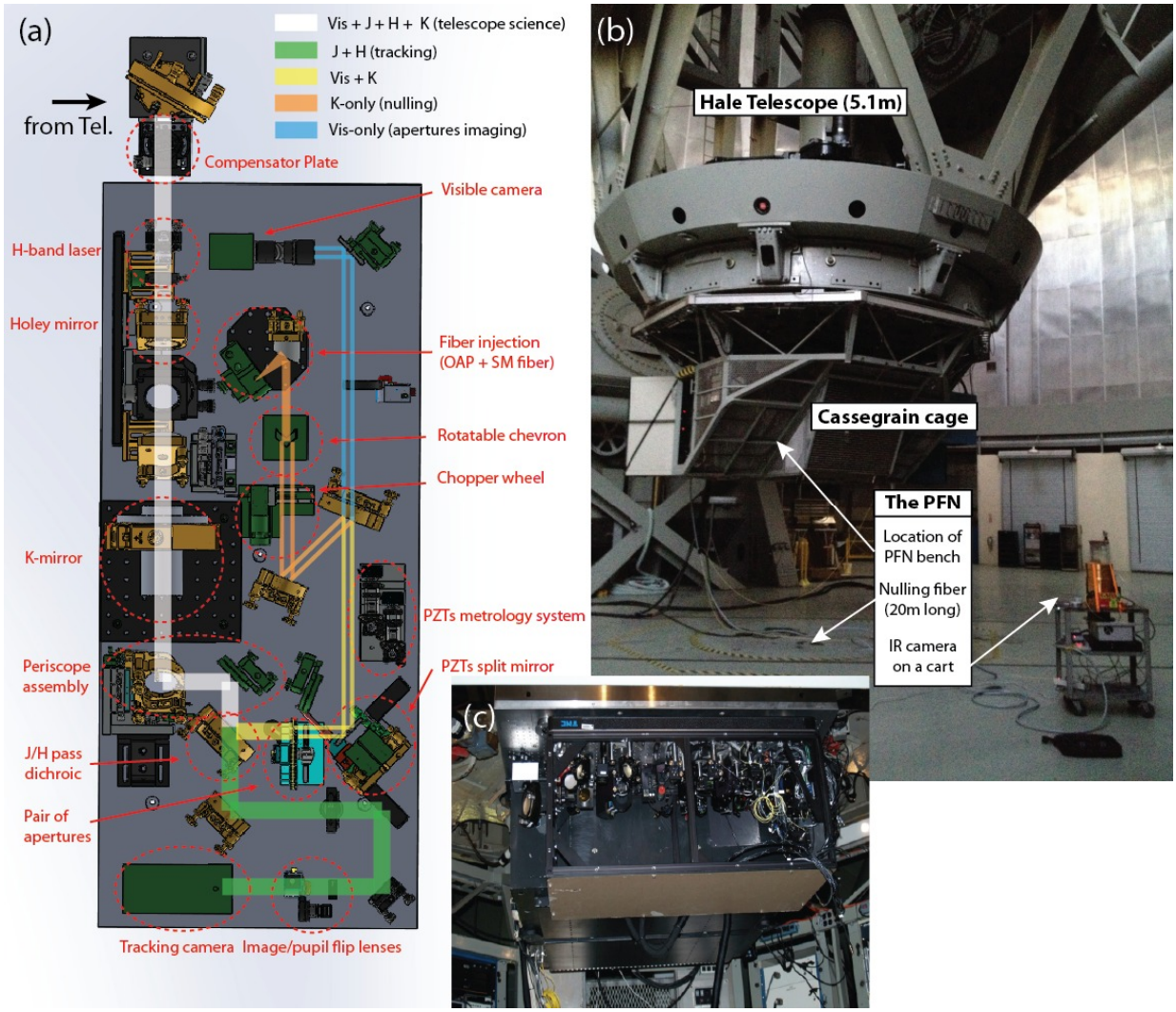

Figure 1. The latest instalment of the PFN instrument on the Palomar 200-inch. (a) Optical layout; (b) Actual observing settings inside the telescope dome; (c) The PFN bench installed upside-down, downstream of the AO system (behind it)

At the SM fiber tip level, all wavefront errors are discarded as transmission losses, and the p3k AO system can be considered as playing the role of a fringe-tracker to maintain the OPD between the two beams around the central "null fringe" (in good seeing, OPD rms across the pupil is typically λ/10). The measured interferometric signal at the fiber output will reach its lowest level (the "null", when OPD = π) from time to time during a recording sequence. Using the chopper wheel to probe the distribution of individual, interferometric and dark signals, this is enough for our Null Self-Calibration Algorithm[15, 16] to be able to retrieve the underlying astrophysical null (see §2.5).

In practice, in the case of an unresolved naked star, or of a uniform disk seen face-on, the measured astrophysical null will be a constant (i.e. no modulation) with baseline rotation, at least down to the measurement accuracy of a ~$2*10^{-4}$. On the other hand, non axi-symmetric source structure, including the presence and position - modulo 180° for the position angle (P.A) - of an off-axis source, will be revealed by a modulation of the null signal as the source flux is modulated by the PFN on-sky transmission (Figure 2).

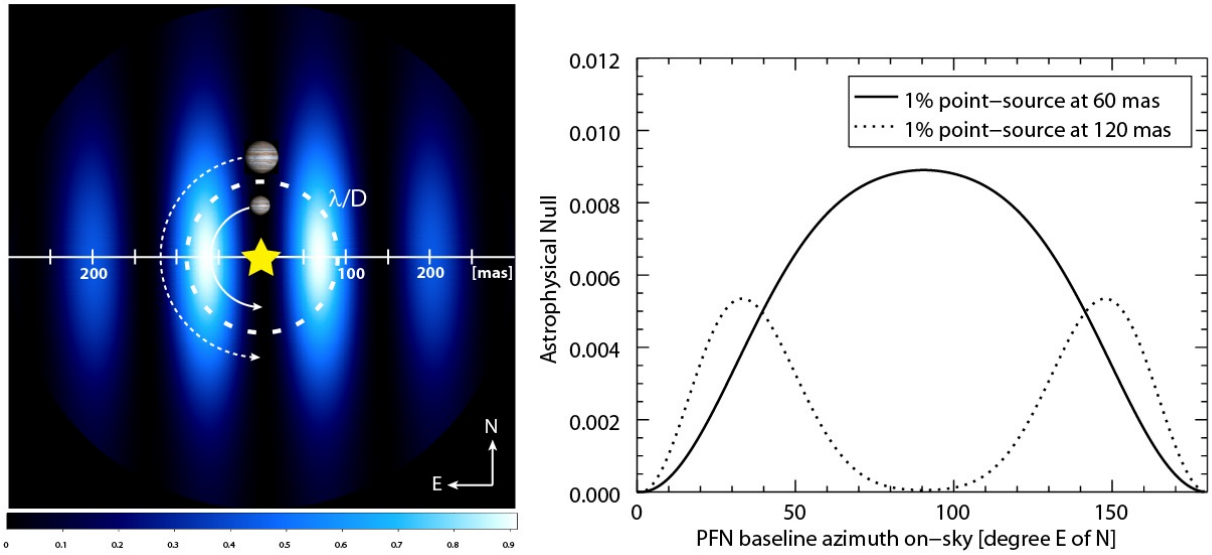

Figure 2. Left: PFN transmission function (fringe pattern) on the sky at Palomar.. Right: Expected astrophysical null in the hypothetical case of point sources carrying 1% of the flux of the unresolved star, and describing the path pictured by the plain and dotted arrows on the left image as the baseline is rotated. The azimuthal modulation frequency provides information on separation, while the position angle can be retrieved from the phase offset (modulo 180°).

2.2 Getting a flat azimuthal null response at Palomar: Compensating the AO dichroic asymmetric dispersion

During the years 2012-3, work was performed to ensure that the instrumental null response at Palomar (using the AO stimulus white light source, or a known naked star on-sky) was maintained below the 0.1% level for all pupil rotation angles. Indeed, it was noticed that the quasi-flat instrumental null level in function of azimuth measured in the laboratory at JPL degraded considerably when the instrument was mounted on the 200-inch Cassegrain cage on-site, even just using the AO white light stimulus: instrumental nulls up to 0.2% were measured at some baselines (Figure 3). This performance loss was caused by the presence of the AO dichroic filter that reflects part of the visible spectrum for wavefront sensing in p3k. Indeed, this dichroic mirror is angled by about 15 degrees off the optical axis in a converging beam path, thus inducing asymmetric chromatic dispersion between the two pupil subapertures when they are not aligned with its principal plane. This dispersion effect reflects into null degradations of the order of 2*10-3 at the worst azimuth angle (Figure 3).

Also taking into account the slight wedge of the AO dichroic filter of 0.015 degrees, we designed a 10-mm thick 1'' diameter "compensator plate" made of Infrasil, located 100 mm upstream of the PFN input focus and sitting at an opposite angle of 11 degree (not 15 degrees, due to the wedge asymmetric glass thickness) relative to the incoming converging beam (Figure 1). ZEMAX® simulations indicated a theoretical limiting null depth of about $1.5*10^{-5}$ with these settings. The compensator plate was then installed upstream of the PFN bench during June 2013, and < $6*10^{-4}$

instrumental null depth was experimentally confirmed for all baseline azimuth angles using the p3k internal white light stimulus source (Figure 3).

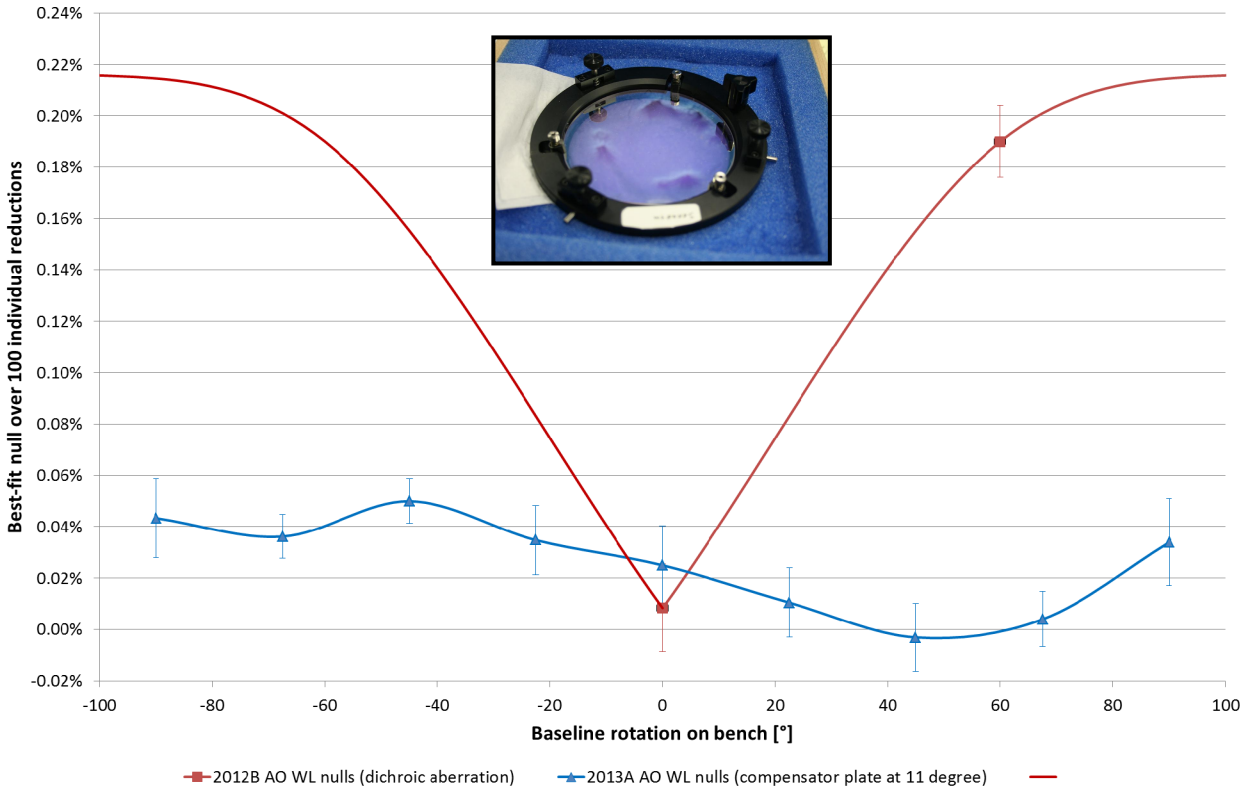

Figure 3. Progress on the correction of the instrumental error vs. azimuth (only at Palomar) caused by the AO dichroic filter over the 2012-2013 time period. The detrimental instrumental null dependence on baseline rotation improves from about 0.2% at the worst azimuth (± 90°) to less than 0.05%. A picture of the AO dichroic filter, set at an angle of 15 degrees off the optical axis, inside a converging beam path, is shown in the inset. However, the best correction is obtained for a compensator plate at 11 degrees, as the asymmetric glass thickness due to the dichroic wedge (0.015 degrees) has also to be compensated for.

2.3 Improvements to the PFN optical layout and new optimized alignment procedure

Several improvements and newly designed beam paths were added over the 2010 version of the PFN bench, in order to facilitate external and internal alignment, and optimal use of the observing time: live compensation of differential tip/tilt drifts, fast baseline azimuth change (less than 5 mn), etc... This notably includes the following new sub-systems:

- Internal H-band pointing laser inserted through a holey fold mirror (the hole matches the 200-inch secondary obscuration) upstream of the K-mirror pupil rotator (Figure 1a): this laser provides an internal alignment reference - independent of any differential motion between the PFN and the AO bench – mostly useful for correcting residual tip/tilt/shear errors induced when using the pupil rotator. This laser beam is also used for initial alignment of the K-mirror. Finally, when the PFN is mounted on the telescope, this H-band beam path represents the reference to align the telescope science beam to.

- Actuated periscope assembly downstream of the K-mirror rotator (Figure 1a): two periscope mirrors are mounted on motorized translation stages to correct for shear errors, and a third actuated fold mirror is used for adjusting pointing. This system is used for 1) initial alignment to the apertures mask, 2) correction of the residual tip/tilt/shear drifts caused by the K-mirror internal alignment errors when it is rotated about its axis.

- H-band tracking imaging path (Figure 1a): a dichroic filter lets the H- (and J-) part of the spectrum reach a PhotonicsScience SWIR InGaAs air-cooled camera, used for tip/tilt or shear tracking. Two lenses mounted on actuated

flip mounts re-image the focal- or pupil-plane, to provide comprehensive tip/tilt and shear tracking capabilities. Such a tracking system serve multiple purposes: 1) initial alignment of the K-mirror using the H-band laser, 2) defining nominal tip/tilt and shear reference centroid positions once the internal alignment beam is aligned to the apertures pair and coupled to the SM fiber downstream, 3) tracking and correcting tip/tilt and shear errors induced by the K-mirror when rotated, using the H-band laser and the actuated 3-mirrors periscope assembly, 4) when on-sky, tracking differential tip/tilt between the PFN and the AO system (caused by the telescope slewing), by measuring the offset from the H-band laser and science beam centroids in pointing mode: this correction is streamed in real-time through remote science-motion commands issued to the p3k AO interface.

- Metrology system for split-mirror piezo-actuators (PZT, Figure 1a): two fiber-coupled green LEDs beams are impending orthogonally to the piezo-split-mirror assembly, and each reflected back to a quad-cell detector. This scheme ensures a genuine piston-move of the PZTs when using them for OPD scan, typically to find the central null fringe. This mode is disabled when using the PZTs to scan tip/tilt for fiber coupling optimization (Scan & Align mode), then new centroids are saved.

2.4 Sensitivity improvements

During the 2011-2012 time period, the PFN infrared detector (at the output of the SM fiber) was upgraded from a single pixel InSb detector to a Nitrogen-cooled IR camera inherited from the decommissioned Palomar Testbed Interferometer (PTI). As a result, sensitivity improvements of about two orders of magnitude were demonstrated in 2012 (Figure 4). This dramatic gain in sensitivity opened a much larger parameter space of targets compared to the initial handful sample of magnitude ~ 1 or brighter stars. Since then, electronics readout upgrades were implemented in 2013-2014, including Correlated Double Sampling (CDS) and multiple reads (typically 3-4 reads). This led to an additional gain of sensitivity of about a factor 3 (Figure 4), currently setting the sensitivity limit of PFN at magnitude ~6 at K-band.

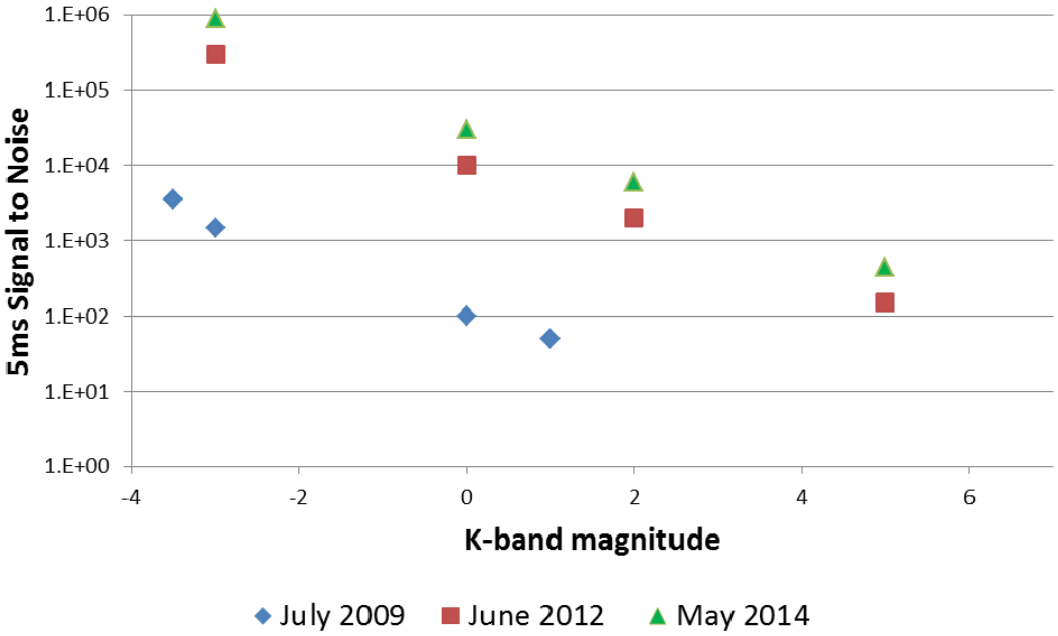

Figure 4. Comparison of previous and current photometric sensitivities: a gain of a factor of ~ 300 has been achieved. The 2009 and 2012 datapoints were measured on-sky, while the 2014 datapoints are extrapolated from lab data.

2.5 Data reduction

A typical single-azimuth observation sequence on-sky consists of a few minutes recording of 2- to 10-ms exposures. The observed signal is constantly chopped at ~12 Hz with a rotating aperture wheel which alternatively lets through the following signals (see Figure 5-Left): flux from sub-aperture "A", sub-aperture "B", both sub-apertures, and dark (both

beams blocked; Martin, et al. 2008). The probability distributions of these different flux signals are the statistically relevant metrics for the astrophysical null, when processed with our null self-calibration algorithm,[15, 16] which retrieves the underlying astrophysical null for each recorded on-sky azimuth. This is achieved by comparing the measured A+B null distribution with different synthetic null distributions built from boot-strapped (i.e. resampled) flux samples of A, B, and dark measurements. Each synthetic null distribution depends solely on 3 parameters (fitted by a Pearson $\chi 2$ minimization): the mean OPD difference between the beams (i.e. the difference from π), the OPD jitter (rms) around that mean, and the astrophysical null N_{as}, which is of course the main quantity of interest (Figure 5-Right). Such best-fit estimates are obtained for 100 different boot-strapped data sequences, in order to evaluate the error bars on the retrieved astrophysical null values. The astrophysical nulls and error bars are derived for each PFN baseline azimuth sampled.

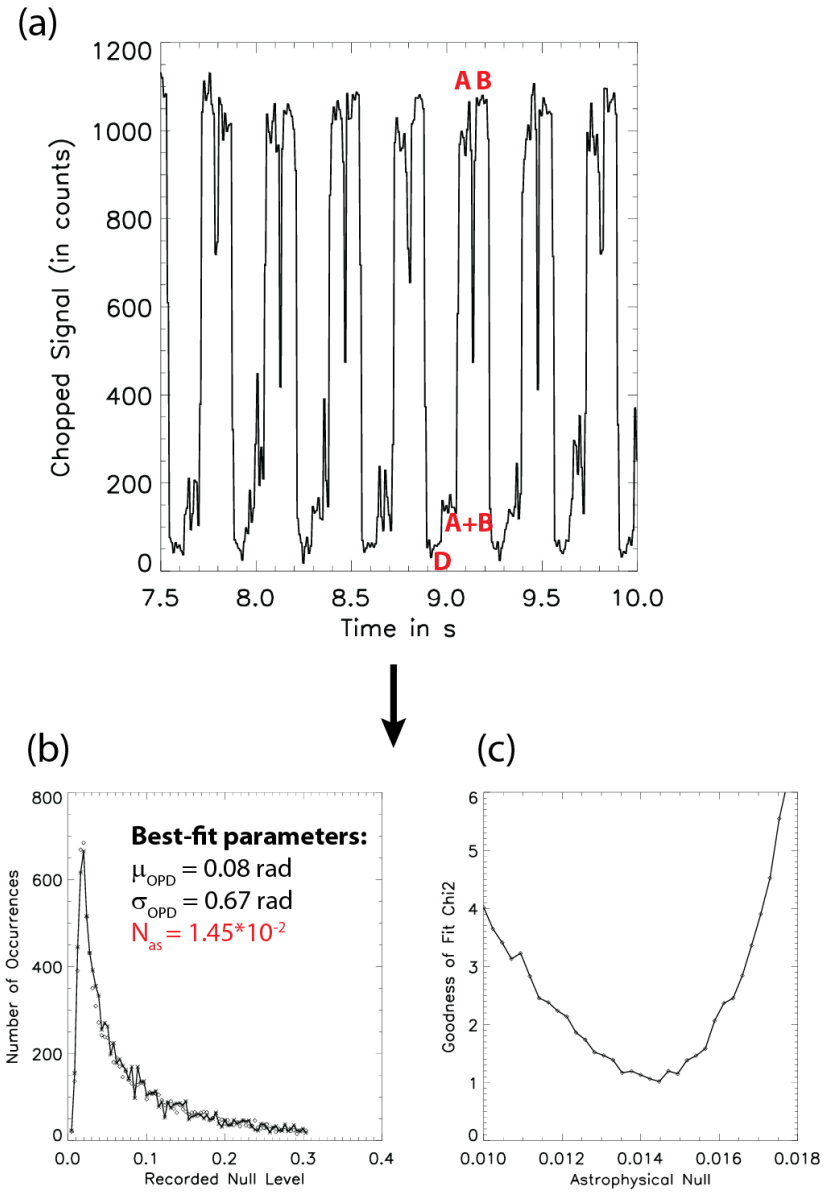

Figure 5. PFN observable quantities on-sky and data reduction. (a): Example of recorded raw chopped signal on-sky, where a different signal is let through every 80 ms, alternating between dark (D), interferometric null (A+B), and individual signals (A and B) states; (b) Example of distribution histogram of experimentally recorded nulls (diamonds); (c) Goodness of fit estimates (Pearson $\chi 2$ minimization) for a variety of synthetic null distributions built from the recorded A and B signals, as a function of underlying astrophysical null. The best fit synthetic histogram is obtained for a $1.45*10^{-2}$ null, and also plotted in (b).

3. SCIENCE WITH THE PFN: OBSERVATION OF AB AURIGAE

3.1 On-sky observation

We observed AB Aur with the PFN in K-band on the night of 2012 October 30 UT, at 6 different azimuth baselines spanning 180° on-sky in steps of 30° (seeing ~ 0.''85). All 6 azimuthal sequence consisted of 300-s long recordings of 10-ms exposures. The resulting reduced astrophysical nulls (see §2.5) for AB Aur are plotted in Figure 6. The figure also displays for comparison the instrumental nulls measured on a combination of calibrator stars and AO internal light source measurements, as the dichroic compensations scheme was only implemented later, in 2013 (§2.2). However, this instrumental null is nearly an order of magnitude smaller than the measured excess leakage around AB Aur. Subtracting this error provides the calibrated astrophysical nulls plotted in Figure 6.

It should be noted that any measured null represents the amount of circumstellar flux leaking through the PFN fringe pattern (Figure 2) divided by the "central flux" unresolved by the PFN. In the case of AB Aur, this unresolved central component corresponds to both the star and any hot dust/gas emission at sub-AU scales (a few mas), as previously reported by Millan-Gabet, *et al.*[11, 12] and Tannirkulam, *et al.*[14] Indeed, this unresolved hot dust/gas emission is believed to dominate over the K-band starlight by at least a factor of two.

Two results are evident looking at Figure 6. First, a 1.52% average null is present at all azimuths. This can be interpreted as the resolved emission detected around AB Aur being dominated by an azimuthally extended source. Second, a less pronounced azimuthal variation on the order of ±0.2% in amplitude can also be observed.

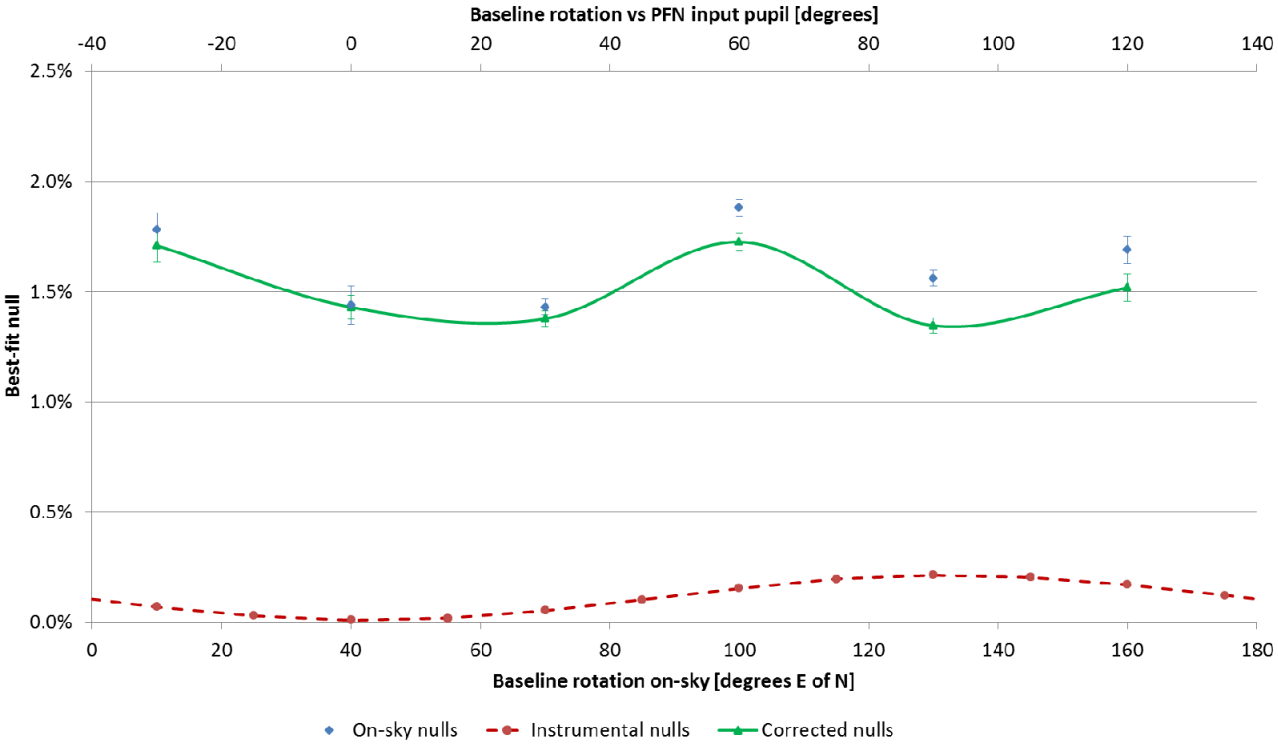

Figure 6. AB Aur on-sky nulls recorded with the PFN on 2012 October 30 UT for six different baselines spanning 150° (180° effectively with the π periodicity of the PFN transmission) azimuthal range by increments of 30°. Subtracting the instrumental nulls (red) from the on-sky nulls (blue) yields the final calibrated astrophysical nulls (green). The green curve is a spline fit to the data (no astrophysical meaning). An average 1.52% null level is observed, with a small ± 0.2% azimuthal modulation.

3.2 Derived constraints on the nature of the emission

Under the hypothesis of AB Aur showing a nearly face-on disk,[7, 17] two scenarios can be considered for the dominant spatially-extended contribution:

- A uniform spatially-extended "halo" filling the PFN FOV. Dividing the measured 1.52% null by the mean PFN transmission over the inner 300 mas (43.2 AU, see Figure 2) - corresponding to 23.6% - yields a total halo flux contributing 6% of the total K-band flux (Figure 7-Left, dashed curve): such an isotropic structure would replicate the observed average null on-sky.

- A ring or narrow annulus type of geometry (multiple rings are also a possibility). Assuming an arbitrarily thin ring, the ring flux as a function of its distance from the star can be derived (Figure 7-Left, plain curve), corresponding the observed mean null. With a single baseline length of 3.2 m, the exact location of this ring-shaped emission cannot be better constrained by the PFN, but realistic flux fractions between 5 and 10% of the total K-band flux would imply a ring separation between 3 and 40 AU (20 and 280 mas)

On the other hand, a variety of contribution could explain the small ±0.2% anisotropic component

- An elliptical ring, or a circular ring, seen at some inclination angle.

- A spiral-type of structure possibly combined with isotropic emission (halo or ring).

- An off-axis point-source in addition to an isotropic emission (halo or ring as the pedestal offset). One can compute a 2D $\chi 2$ plot (Figure 7-Right) mapping the probability that the remaining observed azimuthal null modulation is due to a point source at different locations around AB Aur, and inside the PFN's FOV. The best fit ($\chi 2 = 0.6$) is obtained for a companion at a separation of 122 mas (17.6 AU), P.A = 51° mod 180°, and with a flux of ~ 6.2*10-3 of the unresolved central emission.

- A spatially-extended point-source ("blob"), combined with some isotropic emission. Given the rather large derived flux (6.2*10-3) for the best-fitting point-source (see above), there is a possibility to be in presence of an accreting planet in formation, thus closer to a blob-like geometry.

In summary, although the point source hypothesis is one possible explanation for the observed azimuthal modulation, it is also possible that the origin of this slight anisotropic null signature is caused by a combination of an inclined structure (e.g. a ring) and some disk asymmetry or uneven azimuthal distribution (e.g. spiral arms).

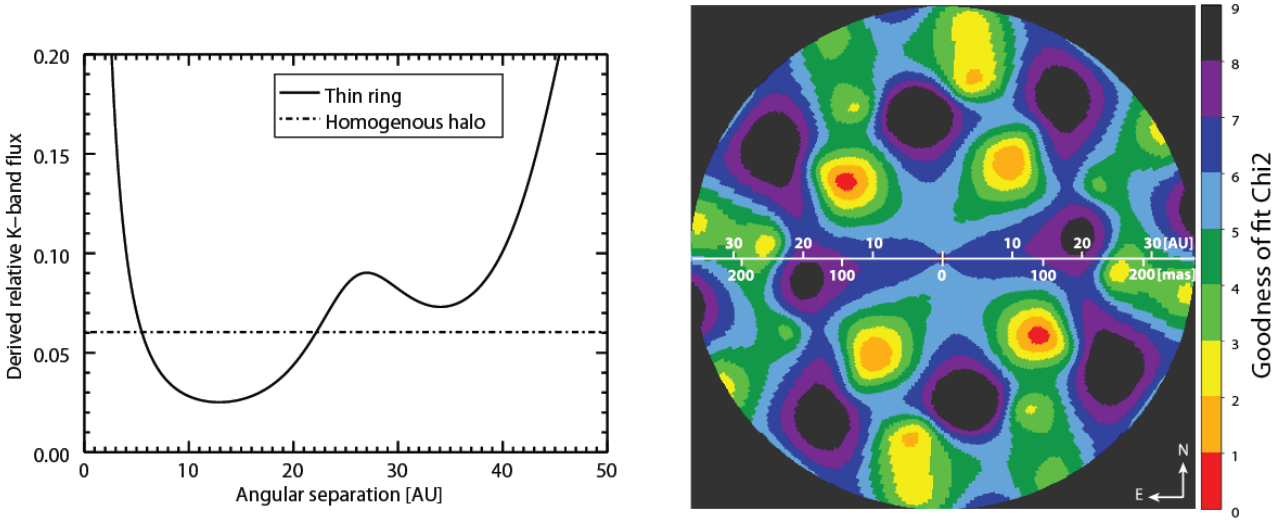

Figure 7. (Left) Derived constraints on the nature of the extended emission responsible for the detected mean null of 1.52%; (Right) χ^2 map showing the most probable location for a companion that could be responsible for the observed ± 0.2% azimuthal modulation of Figure 6. 1 AU = 7 mas at AB Aur distance.

4. CONCLUSIONS AND PERSPECTIVES

The PFN can uniquely explore intermediate angular scales, in-between coronagraphic direct imaging and long-baseline interferometry. The added-value of accessing such a parameter space is well-illustrated in the case of the highly-scrutinized AB Aurigae system, as the PFN field-of-view here directly correspond to the outer solar system planetary region (5-40 AU). We were able to detect a large "excess null" of about 1.52% around AB Aur. This corresponds to a spatially and azimuthally-extended source (halo or ring) contributing ~5 to 10% of the total K-band flux of AB Aur. Furthermore, we measured a ±0.2% azimuthal variation of the null, which could reflect some skewness or anisotropy in the extended source of emission resolved by the PFN, such as, e.g., spiral arm(s) or ellipticity of the ring(s). Alternatively, this small azimuthal signature could also trace the presence of a 0.6%-flux point-source companion, located at ~17.6 AU and P.A = 52° mod 180°.

Over the 2011-2014 time period, the PFN has matured into a full-fledged high-contrast instrument, gaining over a factor ~300 in sensitivity and demonstrating a <6*10-4 azimuthal instrumental null variation over a complete azimuthal rotation. Currently, the PFN is able to observe targets as faint as magnitude ~6 in K-band, and can cover ~6 azimuthal directions on-sky over a 1-hour period, thanks to new semi-automatic alignment sub-systems.

Future upgrades notably encompass a "baseline selector wheel", capable of switching baseline lengths on-the-fly (typical range at Palomar: 2.6 to 3.8 m). Finally we also note that the implementation of such a rotating baseline nuller on a larger telescope will be able to explore nearly AU-scales, even at distances over 100 pc, like in the case of AB Aurigae.

ACKNOWLDGEMENTS

This work was performed at the Jet Propulsion Laboratory, California Institute of Technology, under contract with NASA. The data presented are based on observations obtained at the Hale Telescope, Palomar Observatory, as part of a continuing collaboration between Caltech, NASA/JPL, and Cornell University. We particularly thank the Palomar Observatory and p3k AO staff for their assistance in mounting the PFN and conducting the observations at the Hale Telescope. JK is supported by a Swiss National Science Foundation Advanced Postdoc Mobility fellowship (PA00P2 136416).

REFERENCES

[1] S. Martin, E. Serabyn, K. Liewer, F. Loya, B. Mennesson, C. Hanot and D. Mawet, in *Society of Photo-Optical Instrumentation Engineers (SPIE) Conference Series* (2008), Vol. 7013, pp. 57.

[2] B. Mennesson, C. Hanot, E. Serabyn, K. Liewer, S. R. Martin and D. Mawet, The Astrophysical Journal **743**, 178 (2011).

[3] B. Mennesson, C. Hanot, E. Serabyn, S. R. Martin, K. Liewer, F. Loya and D. Mawet, in *Society of Photo-Optical Instrumentation Engineers (SPIE) Conference Series* (2010), Vol. 7735, pp. 35.

[4] E. Serabyn, B. Mennesson, S. Martin, K. Liewer, D. Mawet, C. Hanot, F. Loya, M. M. Colavita and S. Ragland, in *Society of Photo-Optical Instrumentation Engineers (SPIE) Conference Series* (2010), Vol. 7734, pp. 41.

[5] B. Mennesson, E. Serabyn, C. Hanot, S. R. Martin, K. Liewer and D. Mawet, The Astrophysical Journal **736**, 14 (2011).

[6] L. E. DeWarf, J. F. Sepinsky, E. F. Guinan, I. Ribas and I. Nadalin, The Astrophysical Journal **590**, 357-367 (2003).

[7] M. Fukagawa, M. Hayashi, M. Tamura, Y. Itoh, S. S. Hayashi, Y. Oasa, T. Takeuchi, J. I. Morino, K. Murakawa, S. Oya, T. Yamashita, H. Suto, S. Mayama, T. Naoi, M. Ishii, T. S. Pyo, T. Nishikawa, N. Takato, T. Usuda, H. Ando, M. Iye, S. M. Miyama and N. Kaifu, Astrophys J **605** (1), L53-L56 (2004).

[8] J. Hashimoto, M. Tamura, T. Muto, T. Kudo, M. Fukagawa, T. Fukue, M. Goto, C. A. Grady, T. Henning, K. Hodapp, M. Honda, S. Inutsuka, E. Kokubo, G. Knapp, M. W. McElwain, M. Momose, N. Ohashi, Y. K. Okamoto, M. Takami, E. L. Turner, J. Wisniewski, M. Janson, L. Abe, W. Brandner, J. Carson, S. Egner, M. Feldt, T. Golota, O. Guyon, Y. Hayano, M. Hayashi, S. Hayashi, M. Ishii, R. Kandori, N. Kusakabe, T. Matsuo, S. Mayama, S. Miyama, J.-I. Morino, A. Moro-Martin, T. Nishimura, T.-S. Pyo, H. Suto, R. Suzuki, N. Takato,

H. Terada, C. Thalmann, D. Tomono, M. Watanabe, T. Yamada, H. Takami and T. Usuda, The Astrophysical Journal Letters **729**, L17 (2011).
[9] B. R. Oppenheimer, D. Brenner, S. Hinkley, N. Zimmerman, A. Sivaramakrishnan, R. Soummer, J. Kuhn, J. R. Graham, M. Perrin, J. P. Lloyd, L. C. Roberts, Jr. and D. M. Harrington, The Astrophysical Journal **679**, 1574-1581 (2008).
[10] M. D. Perrin, G. Schneider, G. Duchene, C. Pinte, C. A. Grady, J. P. Wisniewski and D. C. Hines, The Astrophysical Journal Letters **707**, L132-L136 (2009).
[11] R. Millan-Gabet, J. D. Monnier, J.-P. Berger, W. A. Traub, F. P. Schloerb, E. Pedretti, M. Benisty, N. P. Carleton, P. Haguenauer, P. Kern, P. Labeye, M. G. Lacasse, F. Malbet, K. Perraut, M. Pearlman and N. Thureau, The Astrophysical Journal Letters **645**, L77-L80 (2006).
[12] R. Millan-Gabet, F. P. Schloerb, W. A. Traub, F. Malbet, J. P. Berger and J. D. Bregman, Astrophys J **513** (2), L131-L134 (1999).
[13] K. Rousselet-Perraut, M. Benisty, D. Mourard, S. Rajabi, F. Bacciotti, P. Bério, D. Bonneau, O. Chesneau, J. M. Clausse, O. Delaa, A. Marcotto, A. Roussel, A. Spang, P. Stee, I. Tallon-Bosc, H. McAlister, T. Ten Brummelaar, J. Sturmann, L. Sturmann, N. Turner, C. Farrington and P. J. Goldfinger, Astron Astrophys **516**, L1 (2010).
[14] A. Tannirkulam, J. D. Monnier, R. Millan-Gabet, T. J. Harries, E. Pedretti, T. A. ten Brummelaar, H. McAlister, N. Turner, J. Sturmann and L. Sturmann, The Astrophysical Journal Letters **677**, L51-L54 (2008).
[15] C. Hanot, B. Mennesson, S. Martin, K. Liewer, F. Loya, D. Mawet, P. Riaud, O. Absil and E. Serabyn, The Astrophysical Journal **729**, 110 (2011).
[16] C. Hanot, B. Mennesson, E. Serabyn, S. Martin, K. Liewer, F. Loya, D. Mawet, P. Riaud and O. Absil, in *Society of Photo-Optical Instrumentation Engineers (SPIE) Conference Series* (2010), Vol. 7734, pp. 88.
[17] J. A. Eisner, B. F. Lane, R. L. Akeson, L. A. Hillenbrand and A. I. Sargent, The Astrophysical Journal **588**, 360-372 (2003).